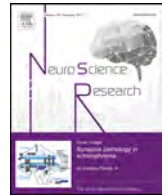




Contents lists available at ScienceDirect

Neuroscience Research

journal homepage: www.elsevier.com/locate/neures



Research Paper

Left, right, or bilateral amygdala activation? How effects of smoothing and motion correction on ultra-high field, high-resolution functional magnetic resonance imaging (fMRI) data alter inferences

Jerry E. Murphy^{a,b,*}, Julio A. Yanes^{a,b}, Lauren A.J. Kirby^{a,b}, Meredith A. Reid^{a,b,c,d}, Jennifer L. Robinson^{a,b,c,d,e}

^a Department of Psychology, 226 Thach Hall, Auburn University, Auburn, AL, 36849, United States

^b Auburn University MRI Research Center, 560 Devall Drive, Auburn, AL, 36849, United States

^c Department of Electrical and Computer Engineering, Auburn University, Auburn, AL, 36849, United States

^d Alabama Advanced Imaging Consortium, United States

^e Center for Neuroscience, Auburn University, AL, 36849, United States

ARTICLE INFO

Article history:

Received 22 May 2018

Received in revised form 28 January 2019

Accepted 31 January 2019

Available online xxx

Keywords:

7T

Amygdala

Preprocessing

Submillimeter resolution

Reproducibility

ABSTRACT

Given the amygdala's role in survival mechanisms, and its pivotal contributions to psychological processes, it is no surprise that it is one of the most well-studied brain regions. One of the common methods for understanding the functional role of the amygdala is the use of functional magnetic resonance imaging (fMRI). However, fMRI tends to be acquired using resolutions that are not optimal for smaller brain structures. Furthermore, standard processing includes spatial smoothing and motion correction which further degrade the resolution of the data. Inferentially, this may be detrimental when determining if the amygdalae are active during a task. Indeed, studies using the same task may show differential amygdala(e) activation. Here, we examine the effects of well-accepted preprocessing steps on whole-brain submillimeter fMRI data to determine the impact on activation patterns associated with a robust task known to activate the amygdala(e). We analyzed 7T fMRI data from 30 healthy individuals collected at sub-millimeter in-plane resolution and used a field standard preprocessing pipeline with different combinations of smoothing kernels and motion correction options. Resultant amygdalae activation patterns were altered depending on which combination of smoothing and motion correction were performed, indicating that whole-brain preprocessing steps have a significant impact on the inferences that can be drawn about smaller, subcortical structures like the amygdala.

Published by Elsevier B.V.

1. Introduction

The amygdalae are almond shaped nuclei embedded in the ventral medial temporal lobes anterior to the hippocampi (see Fig. 1). These small structures play an integral role in many processes that are involved in our survival and key psychological processes. The amygdalae are pivotal for threat assessments linked to phylogenetically preserved survival processes (Fox et al., 2015), and are responsible for integral affective (Hrybowski et al., 2016; Robinson et al., 2010) and cognitive processes such as memory (Guzmán-Vélez et al., 2016), and learning (Farley et al., 2016). Furthermore, the amygdalae are implicated in many psychological disorders such

as posttraumatic stress disorder (Prager et al., 2016), anxiety disorders (Li et al., 2016a), and depression (Connolly et al., 2017), to name a few. Given the breadth of involvement, and the necessity of the amygdala to healthy brain function, it is not surprising that it is one of the most well-studied structures in the human brain.

Commonly, functional magnetic resonance imaging (fMRI) reveals activation patterns associated with specific tasks, which allow investigators to theorize about structure-function relationships. As such, theories regarding lateralization of the amygdalae have become prominent in the literature, and supported by several studies (Robinson et al., 2010; Baeken et al., 2014). Specifically, some theories of amygdala function propose that the right amygdala is associated with response to animal stimuli (Mormann et al., 2011), positive picture encoding (Vasa et al., 2011), and anger (Fulwiler et al., 2012), while the left amygdala is more involved in fear or threat processing (Phelps et al., 2001), processing of

* Corresponding author at: 226 Thach Hall, Department of Psychology, Auburn University, Auburn, AL, 36849, United States.

E-mail address: Jem0058@auburn.edu (J.E. Murphy).

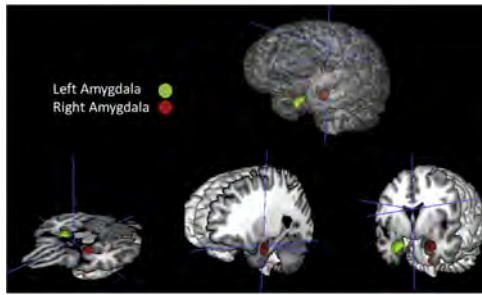


Fig. 1. Location of left and right amygdala in standard MNI space.

emotional arousal and salience (Costanzo et al., 2015), and associative encoding processes (Killgore et al., 2000). Dyck et al. (2011), found evidence for amygdalae lateralization with the left amygdala involved with intentional mood control, and the right amygdala more involved with automatic emotional processing. Baas et al. (2004) provide evidence for functional lateralization of the amygdalae, with results suggesting the left amygdala is more associated with verbal and sustained emotional processing whereas the right amygdala is more associated with visual and dynamic emotional analysis. Robinson et al. (2010) performed a meta-analytic study, and observed distinct functional connectivity differences between the left and right amygdala. Together, these results provide strong evidence for potential lateralization effects.

While fMRI technology allows us to research the function of the amygdala and other structures, it is not without drawbacks. Spatial resolution of lower (i.e. 1.5 or 3T) field strength scanners are not optimal for small brain structures like the amygdalae. Depending on the size of the voxel, the data may contain information from different types of tissue (i.e. grey matter, white matter, or vasculature) sometimes referred to as partial volume effects. The amygdala is particularly vulnerable to partial volume effects based on its location relative to the basal vein of rosenthal which may result in some spurious amygdala activations (Boubela et al., 2015). Regardless of voxel size, and the different types of tissues within, each voxel will also contain “noise” from the scanner, or physiological processes. Additionally, voxels may be large enough to incorporate more than one structure, especially in the case of smaller anatomical structures like the amygdalae. Further complicating this matter, it is standard to preprocess the data, which involves noise reduction steps that ultimately reduce resolution even more. Additionally, whole-brain data acquisition is required if one is concerned about global networks the amygdala may be involved with. As such, we sought to determine how the effects of preprocessing whole-brain fMRI data may affect inferences that can be drawn from data with regard to the amygdala.

The preprocessing of fMRI data converts measurements from each voxel into usable data by transforming, aligning, and correcting the data to allow for further analysis. Ashby (2011) refers to preprocessing as the analyses carried out on the data that are not driven by a specific hypothesis. Currently, there is no “gold standard” preprocessing pipeline (Aurich et al., 2015; Vergara et al., 2016). Many fMRI researchers have started to standardize some aspects of data management and reporting, such as reporting conventions (Nichols et al., 2016), but due to the complexity and variability of fMRI research paradigms there are no hard and fast rules or consensus on critical aspects of data processing.

Regardless of the preprocessing pipeline chosen, researchers often overlook how their choices affect the data. This issue can be exacerbated as technology allows us to increase the acquisition resolution while maintaining a high signal-to-noise ratio, allowing for smaller voxel sizes and more precise measurements of small structures such as amygdalae. Given the novelty of this methodology, it

is unknown how such acquisitions respond to traditional preprocessing steps. To explore the effects of preprocessing at ultra-high resolution, we focus our attention on two steps that effect resolution the most, namely spatial smoothing and motion correction.

Spatial smoothing is the process of assigning each voxel a weighted average value based on neighboring voxels. This can be accomplished by applying a Gaussian kernel to the data resulting in a weighted average for each voxel. This weighted averaging is done mainly to reduce noise (internal and external) without removing the blood oxygen level dependent (BOLD) signal (Jenkinson, 2015), thus increasing signal to noise ratio, but also to allow the data to meet some statistical assumptions and account for slight anatomical differences between participants (Poldrack et al., 2011). However, there are notable drawbacks to smoothing as well. Increasing amounts of smoothing have been demonstrated to “move” activation patterns (Sacchet and Knutson, 2013) or cause clusters of activation to disappear, merge, split, or be created (Fransson et al., 2002; Mikl et al., 2008).

There are several published recommendations for FWHM kernel size. In order to meet statistical assumptions, the recommendations are twice (Poldrack et al., 2011) or three times voxel size (Yue et al., 2010). Mikl et al. (2008) recommended group inference FWHM to be set at 12 mm, sensorimotor cortex at FWHM of 8–10 mm, and smaller structures at 6 mm. The latter recommendation is consistent with a common recommendation that the smoothing kernel be no larger than the area of interest (Poldrack et al., 2011). Given the diversity of strategies for choosing an appropriate FWHM, it is no surprise that there is not a common consensus, and creating a hard and fast rule may not be appropriate. However, it is an important consideration that may have tremendous implications for data analysis.

Smoothing ultra-high-resolution data provides some unique challenges. Sub-millimeter resolution can increase the impact of functional and anatomical variance between participants (White et al., 2001). At lower resolutions, there is a high likelihood that active tissue, non-active tissue, and vasculature are all present in any single voxel. At higher resolutions, there is a greater likelihood that a voxel will contain a more homogenous tissue sample. Therefore, at sub-millimeter resolution, smoothing may average pure active tissue with non-active tissue and ultimately lose the “true” signal. However, there are some benefits to smoothing high resolution data. In a project conducted by Triantafyllou et al. (2006), the authors showed that collecting data at high resolutions and then smoothing the data to a lower resolution does improve the time-course signal to noise ratio.

Another common preprocessing step is motion correction. Motion correction is used to reduce the effect of participant movement while in the scanner. Movement can come from deliberate, conscious movement as participants look around or adjust how they lie; physiological processes like respiration, swallowing, and cardiac rhythm; or movement related to the task. The issue movement causes for fMRI analysis is that voxels are static locations in space, so when a participant moves, brain tissue can move from one voxel location to another. With increased spatial resolution, this can become exacerbated.

There are different methods for motion correction based on strategy and cost function applied to the data, but the overarching process involves computationally aligning volumes of data based on a single reference volume (Ashby, 2011). The various software packages commonly used within the field use different cost functions, but in a study conducted by Oakes et al. (2005) the top software packages produced similar results for motion correction despite different cost functions. In our study, we used motion correction in FMRIB’s Software Library (FSL) (Woolrich et al., 2009), which is accomplished by Motion Correction FMRIB’s Linear Image Registration Tool (MCFLIRT), with options for extended motion

parameters (i.e., standard motion parameters plus their derivatives, and the square of their derivatives) (M. Jenkinson, Bannister, Brady, & Smith, 2002). Standard MCFLIRT uses three levels of a trilinear transformation starting with a coarse 8 mm search followed by two 4 mm searches with increasingly lower tolerances (M. Jenkinson et al., 2002).

Motion correction is an imperfect process. Regardless, motion must be accounted for to increase the accuracy of data. There are studies that examine the different methods of motion correction, such as a study by Parkes et al. (2018) who investigated the efficacy of 19 different approaches to motion correction. There exist various approaches to motion correction likely because of the vast number of variables that may influence the process (e.g., voxel size) and the different types of studies (e.g., resting state fMRI, task-based fMRI, clinical case studies). Additionally, motion correction may effect data differently depending on the type of experimental design (Johnstone et al., 2006). The primary aim of this paper is not to address all of these concerns, but rather to identify, at a basic level, how preprocessing may effect submillimeter fMRI data synergistically with spatial smoothing and how these effects may influence reported amygdala activations.

The preprocessing steps of spatial smoothing and motion correction are known to effect fMRI data, but to date, the extent of their effects on submillimeter fMRI data has not been fully explored. Therefore, we sought to examine the effects these steps have on amygdala activations using submillimeter fMRI data, using a common task known to activate the amygdala (Hariri et al., 2000). We examined the effects of various smoothing kernels and motion correction methods on resultant activation maps. We hypothesized that amygdala activation patterns would be sensitive to both smoothing and motion correction along with other neural structures.

2. Method

We performed high-resolution functional magnetic resonance imaging (hr-fMRI) during completion of a well-known face-matching task, that has had mixed results with regard to amygdala activation (Hariri et al., 2000). Thirty healthy individuals (26 right-handed, 12 males, age $M \pm SD = 21.3 \pm 1.8$) provided informed consent as approved by Auburn University's Independent Review Board (IRB) and were scanned using an optimized EPI sequence (37 slices acquired parallel to the AC-PC line, 0.85 mm x 0.85 mm x 1.5 mm voxels, TR/TE: 3000/28 ms, 70° flip angle, base/phase resolution 234/100, A > P phase encode direction, iPAT GRAPPA acceleration factor = 3, interleaved acquisition, 117 time points, total acquisition time 5:51). Data were acquired on the Auburn University MRI Research Center (AUMRIRC) Siemens 7T MAGNETOM scanner outfitted with a 32-channel head coil by Nova Medical (Wilmington, MA). Prospective motion correction processes were not used during data acquisition. Participants were presented with three stimuli: one stimulus at the top of the screen and two stimuli at the bottom of the screen. The top stimulus was either an angry or fearful face (or a geometric shape, which served as a control condition). The bottom stimuli contained similar faces (or shapes) as the top stimulus with one identical to the top stimulus, or the words "Angry" and "Afraid" to match the top stimulus (e.g., there was a "matching" condition for both faces and shapes, and an additional "labeling" condition for faces). Participants were asked to select the button corresponding to the side of the screen with the matching face/shape or the word that best described the facial expression. Stimuli were presented in blocks of 36 s, with trials lasting 5000 ms, followed by a 1000 ms fixation, for a total of 6 trials per block. Instructional slides (3000 ms) were presented prior to each block (i.e., "match faces", "match forms", "label faces"). Two

blocks each of face matching and labeling were presented, as well as five blocks of geometric shape matching, which served as control conditions with one block of form matching placed between each block of face matching and face labeling and a three second instruction slide between blocks for a total task time of 351 s. For this study, we choose to focus on the contrast Face Matching > Form Matching to use the matching of geometric forms as the control or baseline and the matching of angry or fearful faces as the test condition. Data were analyzed in FSL (Jenkinson et al., 2012) using the FMRIB Expert Analysis Tool (FEAT) version 6.0, with higher-level analyses conducted using FMRIB's Local Analysis of Mixed Effects (FLAME) stage 1 (Beckmann et al., 2003; Woolrich, 2008; Woolrich et al., 2004).

Prior to statistical modeling, data were converted to Neuroimaging Informatics Technology Initiative (NIFTI) format using 'dcm2nii' (Li et al., 2016b) and all non-brain material was removed from the data using FSL's Brain Extraction Tool (BET) (Smith, 2002). Motion outliers were calculated using FSL's motion outlier script function (<http://fsl.fmrib.ox.ac.uk/fsl/fslwiki/FSLMotionOutliers>), which analyzes the data before any preprocessing is done to identify any moderate to large motion beyond what might be correctable with linear motion correction. Motion outliers are identified as those volumes that fall outside the default threshold defined as the 75th percentile + 1.5 * inter-quartile range. The results of running the motion outlier script is a text file identifying volumes exceed the default threshold for motion (in a binary "1"/"0" fashion, where "1" indicates volumes to be excluded). The text file is then included in the statistical analysis as an explanatory variable which regresses out, or excludes, the aberrant volumes from the analysis. Timeseries statistical analysis was carried out using FMRIB's Improved Linear Model (FILM) with local autocorrelation correction, and all functional data were standardized to Montreal Neurological Institute (MNI) space using FMRIB's Linear Image Registration Tool (FLIRT) using the options in FSL of "full search" with 12 degrees of freedom (Jenkinson et al., 2002; Jenkinson and Smith, 2001). Data were smoothed with varying Gaussian kernel sizes (0.0 mm, 1.0 mm, 3.0 mm, 5.0 mm, and 8.0 mm FWHM) to determine the effects of smoothing submillimeter fMRI data.

We also examined various motion correction procedures. The motion correction options within FSL (Jenkinson et al., 2012) allowed us to examine four different levels of motion correction. The first level of motion correct is to not apply any motion correction which we will refer to as no motion correction or NM. The second level of motion correction is standard motion correction as performed by Motion Correction FLIRT (MCFLIRT) (Jenkinson et al., 2002) (a default setting in FSL), which uses the middle volume as an initial template image, and performs an 8 mm search for the motion parameters using the specified cost function. An assumed identity transformation between the middle volume and adjacent volumes is then applied to subsequent volumes. Following the 8 mm search, two additional 4 mm searches are conducted, each using increasingly tighter tolerances with all three optimizations using a trilinear transformation (for more information about how FSL calculates motion correction parameters please go to <https://fsl.fmrib.ox.ac.uk/fsl/fslwiki/MCFLIRT>). We will hereafter refer to the standard or default level of motion correction as MC. The third level includes standard motion correction (MC) along with the explanatory variable of the text file produced by FSL's motion outlier script function (<http://fsl.fmrib.ox.ac.uk/fsl/fslwiki/FSLMotionOutliers>) to exclude volumes with excessive motion outliers from the analysis, which will be hereafter referred to as MC + EV. The fourth level of motion correction we examine includes standard motion correction (MC), with extended motion parameters (standard parameters with their derivatives and squares of the derivatives, which we refer to as AD for added derivatives), and the explanatory variable of motion out-

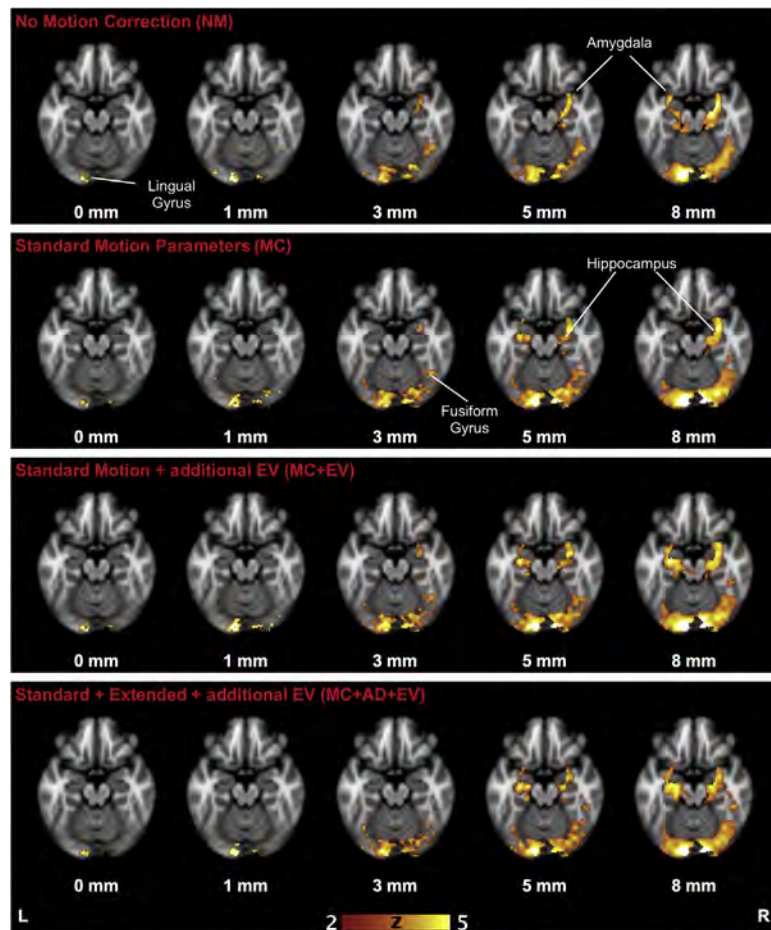


Fig. 2. Results of group analysis for all combinations of smoothing and motion correction.

liers excluded or MC + AD + EV. Each of the above parameters (five levels of smoothing and four levels of motion correction) was parametrically manipulated, with all other preprocessing steps set at default levels except Registration, which we elected to use “Full search” with 12 degrees of freedom. Higher-level analyses were performed with a mixed effects model where subjects were treated as random factors, and images contrasting the “face matching” and “control” conditions were generated. Group Z-statistic images were thresholded on magnitude ($z \geq 2.3$) as well as cluster extent determined by $z > 2.3$ and a corrected cluster significance threshold of $p < 0.05$.

3. Results

Activation clusters varied with the different combinations of smoothing and motion correction. With no smoothing or motion correction (NM at 0 mm) there are only two significant clusters, one centered on the lingual gyrus and one local maximum in the cuneus (see Fig. 2). The combination of MC at 0 mm produces an activation cluster in the right fusiform gyrus that remains at all levels of motion correction at 0 mm, but the cuneus activation disappears at MC and MC + EV, then reappears at MC + AD + EV. With 1 mm smoothing, there is an increase in the number of activated voxels at all levels of motion correction as compared to 0 mm smoothing with the trend continuing with all increases in smoothing levels as described in Table 1. There are some motion correction effects seen at 1 mm smoothing. With NM at 1 mm there is a small bilateral activation in the fusiform gyrus (see Supplemental Material for full report of local maxima). The combination of MC or MC + EV at 1 mm,

only the right fusiform gyrus activation remains. With MC + AD + EV at 1 mm smoothing, the fusiform gyrus activation disappears, and only a small activation cluster around the lingual gyrus remains as shown in Fig. 2.

Smoothing with a 3 mm FWHM kernel resulted in substantially greater activation patterns. As shown in Table 1, and as expected, a 3 mm-FWHM kernel yielded more than 2.5 times the number of statistically significantly activated voxels across all levels of motion correction as compared to a 1 mm voxel. At 3 mm, activations become significant within the left posterior cingulate, right amygdala, and right hippocampus. These three activations are noted at NM at 3 mm, MC at 3 mm, and MC + EV at 3 mm, with an additional activation cluster seen at MC + EV at 3 mm in the left inferior frontal gyrus. Additionally, MC + AD + EV at 3 mm the posterior cingulate activation becomes bilateral, but the amygdala, hippocampus, and inferior frontal gyrus activations no longer reach significance.

As the smoothing kernel increased (e.g., 5 mm and 8 mm kernels), predictably, the number of significant voxels increased. With NM at 5 mm data, results were like the 3 mm kernel, with right amygdala and hippocampal activation. Applying motion correction to 5 mm data produced bilateral activation of the amygdala and hippocampus. The data for NM at 8 mm showed bilateral activation of amygdala and hippocampus, but only right activation of these areas with MC at 8 mm, and bilateral activation at the other levels of motion correction. These latter results are particularly troublesome given that most fMRI studies have employed 5–10 mm kernel sizes, with various levels of motion correction. The inferences regarding amygdala activation in this task then becomes a product of preprocessing choices.

Table 1
Activated voxels and number of clusters for each parametrically matched level of smoothing and motion correction.

	0 mm		1 mm		3 mm		5 mm		8 mm	
	Voxel	Cluster								
NM	261	2	787	3	2563	3	4821	3	7599	4
MC	519	5	1216	4	3475	3	5628	3	7547	1
MC + EV	516	2	1267	3	3681	6	5933	4	8182	3
MC + AD + EV	351	4	891	1	3073	4	5151	3	7143	2

(Description) Number of activated voxels and number of clusters as reported in the standard space cluster list from the FEAT report for each combination of smoothing and motion correction.

4. Discussion

Here, we demonstrate the instability of fMRI activation patterns with heavy implications on inferences by varying two common preprocessing steps: motion correction and smoothing. The magnitude in, and nature of, the differences we found demonstrate that preprocessing choices can greatly influence the inferences drawn from fMRI data, particularly with small structures of interest such as the amygdalae. Our analyses also confirm the effects of spatial smoothing as previously published (Miki et al., 2008) in that activation clusters appear, disappear, merge, or split as changes in FWHM are made while motion correction remains constant. The same pattern held true for activation clusters - as the level of motion correction changed with FWHM remaining constant. For example, NM at 8 mm resulted in significant bilateral activations of the amygdala and hippocampus, but only right activation of amygdala and hippocampus were identified with MC at 8 mm. The combination of MC + EV at 8 mm returned the bilateral activation, which remained the same for MC + AD + EV at 8 mm.

The effects of spatial smoothing seem to be rather consistent across participants, but the effects of motion correction are particular to the extent of motion within each participant. Fig. 3 shows data from two participants. Participant A had relatively little motion compared to Participant B, as indicated by the MCFLIRT estimated mean displacement charts. For Participant A, there are only minor changes to the activation maps across the different levels of motion correction due to the relatively small amount of movement from the participant. Participant B, however, shows large changes in activation patterns as levels of motion correction change. Additionally, there were 16 volumes identified as motion outliers for Participant B with only 6 identified for Participant A. Given that these data are from healthy adults, the problem could be substantially exacerbated in populations prone to motion (i.e., older adults, younger children). Thus, the effects of smoothing can be generalized, but the effects of motion correction are dependent on individual variations within the data. Acquisitions at 7T or higher field strengths which allow for smaller voxels will likely exacerbate the issues of motion during a scan and may explain why changes in motion correction in this study resulted in such dramatic differences.

Differences in fMRI data preprocessing are confounds that are difficult to account for, yet our data suggest that they have robust effects on activation-level results. In our study, we noted different results for amygdala activation based on different combinations of smoothing and motion correction with either none, right, or bilateral activations of the amygdala(e). These differences would ultimately lead to different inferences pertaining to the function and possible lateralization of the amygdalae. Furthermore, such a finding may have trickle down effects for meta-analyses based on neuroimaging databases which rely on coordinates of activation (Robinson et al., 2015, 2012; Robinson et al., 2010). We also note that traditional recommendations for smoothing of fMRI data may need to be revisited for ultra-high resolution data. These results suggest that preprocessing choices may contribute to the current reproducibility crisis (Earp and Everett, 2015; Poldrack and Poline, 2015).

The task chosen for this project was one known to activate the amygdala (Hariri et al., 2000). The data for the Hariri et al. (2000) article were collected on a 3 T scanner with 4 mm slices with 1 mm gap. They report using motion correction and a FWHM kernel of 6 mm to smooth their data (Hariri et al., 2000). In the original article, Hariri et al. (2000), using the same contrast used for this project (i.e., affective face matching vs. control), reported activation of bilateral amygdala, right thalamus, and right fusiform gyrus. We demonstrate concordant results with MC at 5 mm. The combination of MC at 5 mm, we see local maxima in the right amygdala (there are activated voxels in the left amygdala as well, but the left amygdala is not listed in local maxima) and right thalamus, but instead of right fusiform gyrus, our data report the local maximum in the left fusiform gyrus. The amygdala activation in our data does not appear until 3 mm smoothing or 3.5 times our voxel size with the activation being none, left, right, or bilateral depending on the combination of smoothing and motion correction (Fig. 2).

The decisions regarding preprocessing have direct effects on inferences drawn from fMRI data but the totality of the effects may not always be evident. Without applying motion correction (NM), we see right amygdala activation NM at 5 mm that becomes bilateral with NM at 8 mm. The opposite is true with MC at 5 mm where activation is bilateral but only right activation with MC at 8 mm (Fig. 2). This curious result prompted a *post hoc* analysis of the BOLD signal time series for the right and left amygdala. The right and left amygdala time series data for the four combinations (NM at 5 mm; NM at 8 mm; MC at 5 mm; MC at 8 mm) provide no evidence for why activation patterns would change from lateral to bilateral (Fig. 4). One possible explanation for the activation changes noted is that FSL does use Gaussian random field theory (RFT) for cluster thresholding where smoothing is an integral aspect of determining statistical significance (Li et al., 2014, 2015). It is also possible that the different smoothing levels may have effected cluster significance, or the effects of partial volumes for smaller structures like the amygdala become more pronounced at different smoothing levels causing changes in lateral to bilateral activations even though time series data shows left and right amygdala are activating together.

The Hariri et al. (2000) task has been used by several research groups because of its robust amygdala activation. Most of the published articles using the task (e.g., Gaebler et al., 2013; Mattson et al., 2016; van Wingen et al., 2011) reported similar results to Hariri et al. (2000), but others have reported differential activation patterns specifically for the amygdala and hippocampus (Contreras-Rodríguez et al., 2014; Fagundo et al., 2014; Wang et al., 2004). Table 2 shows a selection of articles with their findings for limbic activation in addition to the preprocessing steps that were applied to the data, activations reported, motion correction information if described, the FWHM smoothing kernel used, spatial resolution if information was published, and scanner field strength. Our results, in combination with previous data on this task, highlight the necessity to understand the effects of preprocessing on whole-brain functional imaging data, given the array of inferences that one would draw from right, left, or bilateral amygdala activation, and the subsequent theoretical models developed because of these inferences.

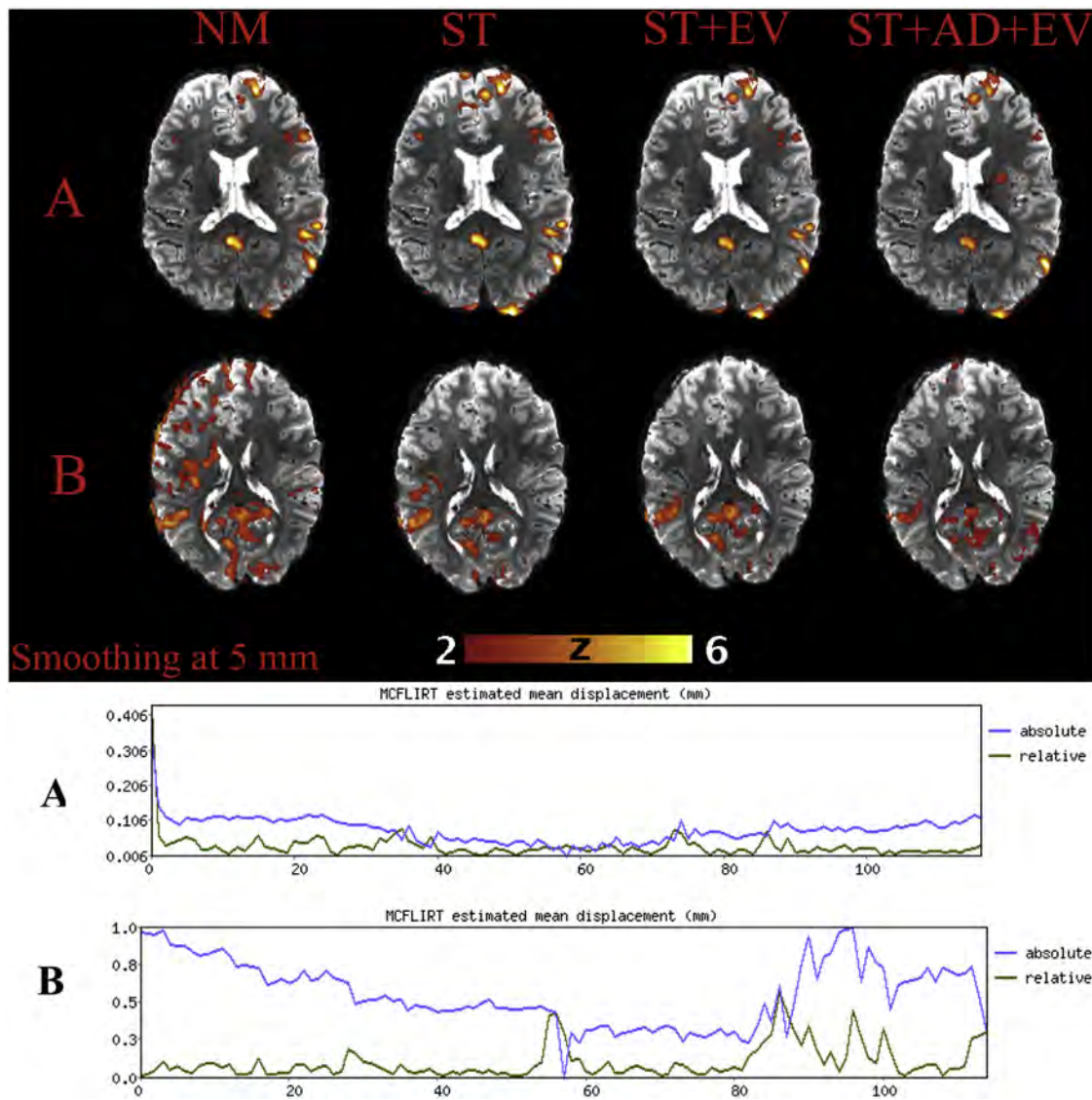


Fig. 3. Activation maps for two participants are shown for the levels of motion correction at 5 mm smoothing along with the motion estimated mean displacement charts for each. Participant A had very little motion resulting in very little difference in activation maps for the different levels of motion correction. Participant B had much more movement resulting in large changes in activations and the significance of the activations as levels of motion correction change.

Table 2
Reported activations of Amygdala and Hippocampus from a sample of articles using Hariri et al. (2000) task.

Article	Reported activations		Motion correction	FWHM	Resolution	Scanner
	Amygdala	Hippocampus				
Hariri et al. (2000)	Bilateral	No mention	Standard	6 mm	4 mm slice thickness**	3T
Gaebler et al. (2013)	Bilateral	No mention	Motion Scrubbing	6 mm	3 mm slice thickness**	3T
van Wingen et al. (2011)	Bilateral	Bilateral	Realign to 1st volume	8 mm	3.5 × 3.5 × 3 mm	1.5T
Mattson et al. (2016)	Bilateral	No mention	Regressing out outliers (>2 mm or 2°)	6 mm	3 × 3 × 3 mm	3T
Contreras-Rodríguez et al. (2014)	Right	Bilateral	Standard	8 mm	3.75 × 3.73 × 4 mm	1.5T
Wang et al. (2004)	Right	Right	Motion Scrubbing	6 mm	3.1 × 3.1 × 4 mm	3T
Fagundo et al. (2014)	Left*	No mention	No mention	8 mm	3.75 × 3.75 × 4 mm	1.5T

(Description and note) A selection of articles that used the Hariri et al. (2000) task that reported a contrast of “Matching versus Control.” Amygdala and hippocampus activations vary among articles. The first two articles did not report field of view (FOV) or matrix size so voxel dimensions could not be calculated. *The Fagundo et al., 2014 paper reported only 2 voxels in left amygdala active at pre-treatment, with no activation of amygdala at post-treatment. **Only slice thickness was reported in these articles.

5. Limitations

The major limitation of this study is that the true amygdala activation is unknown, making any specific recommendation for motion correction and spatial smoothing parameters to use with high-resolution data inadvisable. We also did not take any steps to

process the data to focus only on the amygdala as one might if only a single region of interest (ROI) is the focus. Instead we examined preprocessing as one would for whole brain data commensurate with many studies that look for amygdala activation as part of a larger study question as is the case in PTSD research. Additionally, we choose to keep other preprocessing steps at the default setting

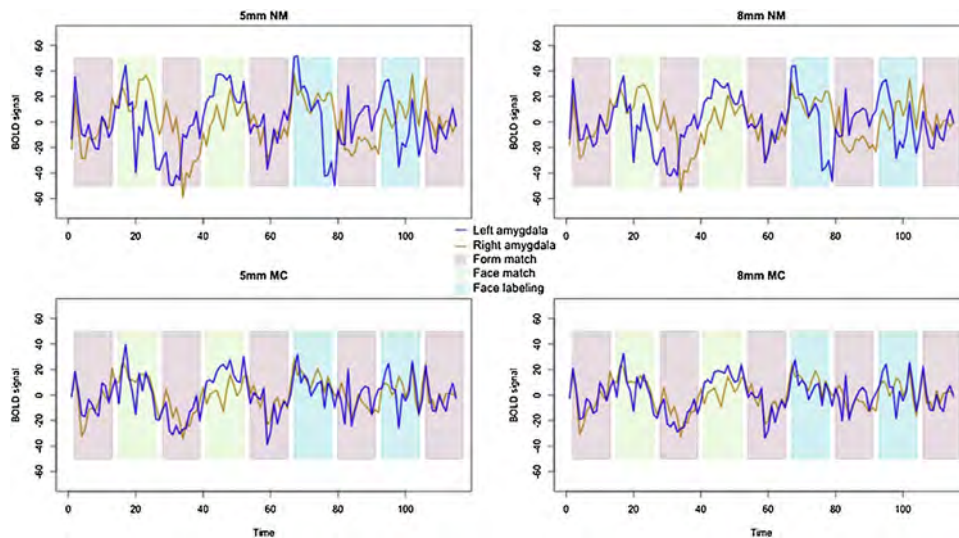


Fig. 4. Time series data for left and right amygdala for each combination of smoothing and motion correction as labeled. Bold signal time series was averaged across all 30 participants and then de-meant for ease of comparisons. The Y axis is the de-meant Bold signal with the X axis time during the task. The task conditions are superimposed on the graph with pink representing Form matching that served as the control condition and the light green is the Face matching condition which was our test condition. The light blue was Face naming and was not used as a contrast for this study (For interpretation of the references to colour in this figure legend, the reader is referred to the web version of this article.).

to include registration with the standard MNI-152 brain template, Z stat thresholds, and temporal filtering. These other preprocessing steps may ultimately influence activations reported, our focus was only on manipulating FWHM kernel size and motion correction parameters.

6. Conclusion

The amygdalae are integral structures to many affective and perceptual process. The results from the current study should serve as a cautionary tale to researchers about the consequences fMRI data preprocessing choices have on amygdala activations as well as other small structures, which may profoundly affect the inferences drawn from a given data set. Furthermore, these results provide insight into the effects of preprocessing on submillimeter fMRI acquisition. Understanding the effects of preprocessing on higher resolution will become increasingly important as advances in neuroimaging support more frequent use of high-resolution scan sequences. Given that mixed results have, unfortunately, been a hallmark feature of the neuroimaging community (for a variety of reasons, including the lack of statistical rigor), it is critical that we work towards a better understanding of how our subjective decisions in preprocessing pipelines can substantially impact our results specifically as they pertain to small structures like the amygdalae. Technological advances will continue to push the limits of spatial and temporal resolution allowing for laminar and columnar specificity (Vu et al., 2017). Researchers should critically consider the effects that these advancements will have on data and processing streams as the benefits from technological and methodological advancements may be washed out by using conventional preprocessing parameters. We should not assume that “standard” preprocessing of data used at lower resolutions should be blindly applied to ultra-high field, high resolution data. It is also not expedient, or possibly ethical, to run data through multiple preprocessing parameters to search for a specific result.

We cannot recommend a specific combination of smoothing and motion correction parameters based on this study alone as each study will have idiosyncrasies that will need to be considered. Investigators need to carefully consider the ROI, the spatial

resolution of their data, and their participant population. We do recommend that preprocessing parameters be chosen *a priori*, taking into account the size of the main structures of interest and the total effect that smoothing and motion correction will have on data. Our data point towards more rigorous motion correction yielding less spurious activation patterns, while smoothing is still important for capturing signal from smaller ROIs, despite more voxels in the ROI due to the increased resolution. The overarching aim of this study is to illuminate the effects of preprocessing on inferences drawn from the data specifically, but also to add to the conversation concerning the reproducibility issues in fMRI research. Additional research should be conducted to determine whether the patterns of results we identified are affected by changes in acquisition parameters, post-processing software packages, or scanning sequences.

7. Context paragraph

This project was born out of questions within our lab on what preprocessing parameters should be used on the Siemens 7T data. The project began with taking a subsample of data and analyzing it with a couple different parameters. The results shocked us in that small changes resulted in large activation changes within the data. The next obvious step was to take a full dataset and systematically investigate the effects of preprocessing parameters, specifically looking at spatial smoothing and motion correction. The results were shared within our department and presented at a local research symposium. The questions and interest generated by others sparked the writing of this article. The aim is not to make any concrete recommendations for preprocessing 7T data, but to illustrate the effects. As our ability to collect higher and higher resolution fMRI data improves, we need to continually test out how preprocessing steps are effecting the data. Researchers should consider the results of this project and evaluate the preprocessing decisions they make.

Funding

This research did not receive any specific grant from funding agencies in the public, commercial, or not-for-profit sectors.

Appendix A. Supplementary data

Supplementary material related to this article can be found, in the online version, at doi:<https://doi.org/10.1016/j.neures.2019.01.009>.

References

- Ashby, F.G., 2011. *Statistical Analysis of fMRI Data*. The MIT Press, Cambridge Massachusetts.
- Aurich, N.K., Alves Filho, J.O., Marques da Silva, A.M., Franco, A.R., 2015. Evaluating the reliability of different preprocessing steps to estimate graph theoretical measures in resting state fMRI data. *Front. Neurosci.* 9, 48, <http://dx.doi.org/10.3389/fnins.2015.00048>.
- Baas, D., Aleman, A., Kahn, R.S., 2004. Lateralization of amygdala activation: a systematic review of functional neuroimaging studies. *Brain Res. Rev.* 45 (2), 96–103, <http://dx.doi.org/10.1016/j.brainresrev.2004.02.004>.
- Baeken, C., Marinazzo, D., Van Schuerbeek, P., Wu, G.-R., De Mey, J., Luybaert, R., De Raedt, R., 2014. Left and right amygdala–medial frontal cortical functional connectivity is differentially modulated by harm avoidance. *PLoS One* 9 (4).
- Beckmann, C., Jenkinson, M., Smith, S.M., 2003. General multi-level linear modelling for group analysis in FMRI. *NeuroImage* 20, 1052–1063.
- Boubela, R.N., Kalcher, K., Huf, W., Seidel, E.-M., Derntl, B., Pezawas, L., et al., 2015. fMRI measurements of amygdala activation are confounded by stimulus correlated signal fluctuation in nearby veins draining distant brain regions. *Sci. Rep.* 5, 10499, <http://dx.doi.org/10.1038/srep10499>, supplementary-information <https://www.nature.com/articles/srep10499>.
- Connolly, C.G., Ho, T.C., Blom, E.H., LeWinn, K.Z., Sacchet, M.D., Tymofiyeva, O., et al., 2017. Resting-state functional connectivity of the amygdala and longitudinal changes in depression severity in adolescent depression. *J. Affect. Disord.* 207, 86–94, <http://dx.doi.org/10.1016/j.jad.2016.09.026>.
- Contreras-Rodríguez, O., Pujol, J., Batalla, I., Harrison, B.J., Bosque, J., Ibern-Regàs, I., et al., 2014. Disrupted neural processing of emotional faces in psychopathy. *Soc. Cogn. Affect. Neurosci.* 9 (4), 505–512.
- Costanzo, E.Y., Villarreal, M., Drucaroff, L.J., Ortiz-Villafañe, M., Castro, M.N., Goldschmidt, M., et al., 2015. Hemispheric specialization in affective responses, cerebral dominance for language, and handedness: lateralization of emotion, language, and dexterity. *Behav. Brain Res.* 288, 11–19, <http://dx.doi.org/10.1016/j.bbr.2015.04.006>.
- Dyck, M., Loughhead, J., Kellermann, T., Boers, F., Gur, R.C., Mathiak, K., 2011. Cognitive versus automatic mechanisms of mood induction differentially activate left and right amygdala. *NeuroImage* 54 (3), 2503–2513, <http://dx.doi.org/10.1016/j.neuroimage.2010.10.013>.
- Earp, B.D., Everett, J.A., 2015. *How to Fix Psychology's Replication Crisis*. The Chronicle of Higher Education.
- Fagundo, A.B., Via, E., Sánchez, I., Jiménez-Murcia, S., Forcano, L., Soriano-Mas, C., et al., 2014. Physiological and brain activity after a combined cognitive behavioral treatment plus video game therapy for emotional regulation in bulimia nervosa: a case report. *J. Med. Internet Res.* 16 (8), e183, <http://dx.doi.org/10.2196/jmir.3243>.
- Farley, S.J., Radley, J.J., Freeman, J.H., 2016. Amygdala modulation of cerebellar learning. *J. Neurosci.* 36 (7), 2190–2201, <http://dx.doi.org/10.1523/JNEUROSCI.3361-15.2016>.
- Fox, A.S., Oler, J.A., Tromp, D.P.M., Fudge, J.L., Kalin, N.H., 2015. Extending the amygdala in theories of threat processing. *Trends Neurosci.* 38 (5), 319–329, <http://dx.doi.org/10.1016/j.tins.2015.03.002>.
- Fransson, P., Merboldt, K.-D., Petersson, K.M., Ingvar, M., Frahm, J., 2002. On the effects of spatial filtering—a comparative fmri study of episodic memory encoding at high and low resolution. *NeuroImage* 16 (4), 977–984, <http://dx.doi.org/10.1006/nimg.2002.1079>.
- Fulwiler, C.E., King, J.A., Zhang, N., 2012. Amygdala–orbitofrontal resting-state functional connectivity is associated with trait anger. *NeuroReport: Rapid Commun. Neurosci. Res.* 23 (10), 606–610, <http://dx.doi.org/10.1097/WNR.0b013e3283551cfc>.
- Gaebler, M., Daniels, J.K., Lamke, J.-P., Fydrich, T., Walter, H., 2013. Heart rate variability and its neural correlates during emotional face processing in social anxiety disorder. *Biol. Psychol.* 94 (2), 319–330, <http://dx.doi.org/10.1016/j.biopsycho.2013.06.009>.
- Guzmán-Vélez, E., Warren, D.E., Feinstein, J.S., Bruss, J., Tranel, D., 2016. Dissociable contributions of amygdala and hippocampus to emotion and memory in patients with alzheimer's disease. *Hippocampus* 26 (6), 727–738, <http://dx.doi.org/10.1002/hipo.22554>.
- Hariri, A.R., Bookheimer, S.Y., Mazziotta, J.C., 2000. Modulating emotional responses: effects of a neocortical network on the limbic system. *NeuroReport* 11 (1), 43–48.
- Hrybouski, S., Aghamohammadi-Sereshtki, A., Madan, C.R., Shafer, A.T., Baron, C.A., Seres, P., et al., 2016. Amygdala subnuclei response and connectivity during emotional processing. *NeuroImage* 133, 98–110, <http://dx.doi.org/10.1016/j.neuroimage.2016.02.056>.
- Jenkinson, M., Retrieved from <http://fsl.fmrib.ox.ac.uk/fsl/fslwiki/FEAT/UserGuide-Pre-Stats> 2015. *FEAT/UserGuide*.
- Jenkinson, M., Smith, S.M., 2001. A global optimisation method for robust affine registration of brain images. *Med. Image Anal.* 5 (2), 143–156.
- Jenkinson, M., Bannister, P., Brady, J.M., Smith, S.M., 2002. Improved optimisation for the robust and accurate linear registration and motion correction of brain images. *NeuroImage* 17 (2), 825–841.
- Jenkinson, M., Beckmann, C.F., Behrens, T.E., Woolrich, M.W., Smith, S.M., 2012. FSL. *NeuroImage* 62, 782–790.
- Johnstone, T., Ores Walsh, K.S., Greischar, L.L., Alexander, A.L., Fox, A.S., Davidson, R.J., Oakes, T.R., 2006. Motion correction and the use of motion covariates in multiple-subject fMRI analysis. *Hum. Brain Mapp.* 27 (10), 779–788, <http://dx.doi.org/10.1002/hbm.20219>.
- Killgore, W.D.S., Casasanto, D.J., Yurgelun-Todd, D.A., Maldjian, J.A., Detre, J.A., 2000. Functional activation of the left amygdala and hippocampus during associative encoding. *NeuroReport: Rapid Commun. Neurosci. Res.* 11 (10), 2259–2263, <http://dx.doi.org/10.1097/00001756-200007140-00039>.
- Li, H., Nickerson, L.D., Xiong, J., Zou, Q., Fan, Y., Ma, Y., et al., 2014. A high performance 3D cluster-based test of unsmoothed fMRI data. *NeuroImage* 98 (Supplement C), 537–546, <http://dx.doi.org/10.1016/j.neuroimage.2014.05.015>.
- Li, H., Nickerson, L.D., Zhao, X., Nichols, T.E., Gao, J.-H., 2015. A voxelation-corrected non-stationary 3D cluster-size test based on random field theory. *NeuroImage* 118 (Supplement C), 676–682, <http://dx.doi.org/10.1016/j.neuroimage.2015.05.094>.
- Li, W., Cui, H., Zhu, Z., Kong, L., Guo, Q., Zhu, Y., et al., 2016a. Aberrant functional connectivity between the amygdala and the temporal pole in drug-free generalized anxiety disorder. *Front. Hum. Neurosci.* 10.
- Li, X., Morgan, P.S., Ashburner, J., Smith, J., Rorden, C., 2016b. The first step for neuroimaging data analysis: DICOM to Nifti conversion. *J. Neurosci. Methods* 264, 47–56.
- Mattson, W.I., Hyde, L.W., Shaw, D.S., Forbes, E.E., Monk, C.S., 2016. Clinical neuro-prediction: Amygdala reactivity predicts depressive symptoms 2 years later. *Soc. Cogn. Affect. Neurosci.* 11 (6), 892–898, <http://dx.doi.org/10.1093/scan/nsw018>.
- Mikl, M., Mareček, R., Hlušík, P., Pavlicová, M., Drastich, A., Chlebus, P., et al., 2008. Effects of spatial smoothing on fMRI group inferences. *Magn. Reson. Imaging* 26 (4), 490–503, <http://dx.doi.org/10.1016/j.mri.2007.08.006>.
- Mormann, F., Dubois, J., Kornblith, S., Milosavljevic, M., Cerf, M., Ison, M., et al., 2011. A category-specific response to animals in the right human amygdala. *Nat. Neurosci.* 14 (10), 1247–1249, <http://dx.doi.org/10.1038/nn.2899>.
- Nichols, T.E., Das, S., Eickhoff, S.B., Evans, A.C., Glatard, T., Hanke, M., et al., 2016. Best practices in data analysis and sharing in neuroimaging using MRI. *bioRxiv*, 054262.
- Oakes, T.R., Johnstone, T., Ores Walsh, K.S., Greischar, L.L., Alexander, A.L., Fox, A.S., Davidson, R.J., 2005. Comparison of fMRI motion correction software tools. *NeuroImage* 28 (3), 529–543, <http://dx.doi.org/10.1016/j.neuroimage.2005.05.058>.
- Parkes, L., Fulcher, B., Yücel, M., Fornito, A., 2018. An evaluation of the efficacy, reliability, and sensitivity of motion correction strategies for resting-state functional MRI. *NeuroImage* 171, 415–436, <http://dx.doi.org/10.1016/j.neuroimage.2017.12.073>.
- Phelps, E.A., O'Connor, K.J., Gatenby, J.C., Gore, J.C., Grillon, C., Davis, M., 2001. Activation of the left amygdala to a cognitive representation of fear. *Nat. Neurosci.* 4 (4), 437–441, <http://dx.doi.org/10.1038/86110>.
- Poldrack, R.A., Poline, J.-B., 2015. The publication and reproducibility challenges of shared data. *Trends Cogn. Sci. (Regul. Ed.)* 19 (2), 59–61, <http://dx.doi.org/10.1016/j.tics.2014.11.008>.
- Poldrack, R.A., Mumford, J.A., Nichols, T.E., 2011. *Handbook of Functional MRI Data Analysis*. Cambridge University Press, New York, NY.
- Prager, E.M., Wynn, G.H., Ursano, R.J., 2016. The tenth annual amygdala, stress, and PTSD conference: 'The amygdala: dysfunction, hyperfunction, and connectivity'. *J. Neurosci. Res.* 94 (6), 433–436, <http://dx.doi.org/10.1002/jnr.23742>.
- Robinson, J.L., Laird, A.R., Glahn, D.C., Lovallo, W.R., Fox, P.T., 2010. Metaanalytic connectivity modeling: delineating the functional connectivity of the human amygdala. *Hum. Brain Mapp.* 31 (2), 173–184.
- Robinson, J.L., Laird, A.R., Glahn, D.C., Blangero, J., Sanghera, M.K., Pessoa, L., et al., 2012. The functional connectivity of the human caudate: an application of meta-analytic connectivity modeling with behavioral filtering. *NeuroImage* 60 (1), 117–129, <http://dx.doi.org/10.1016/j.neuroimage.2011.12.010>.
- Robinson, J.L., Barron, D.S., Kirby, L.A.J., Bottenhorn, K.L., Hill, A.C., Murphy, J.E., et al., 2015. Neurofunctional topography of the human hippocampus. *Hum. Brain Mapp.* 36 (12), 5018–5037, <http://dx.doi.org/10.1002/hbm.22987>.
- Sacchet, M.D., Knutson, B., 2013. Spatial smoothing systematically biases the localization of reward-related brain activity. *NeuroImage* 66, 270–277, <http://dx.doi.org/10.1016/j.neuroimage.2012.10.056>.
- Smith, S.M., 2002. Fast robust automated brain extraction. *Hum. Brain Mapp.* 17 (3), 143–155.
- Triantafyllou, C., Hoge, R.D., Wald, L.L., 2006. Effect of spatial smoothing on physiological noise in high-resolution fMRI. *NeuroImage* 32 (2), 551–557, <http://dx.doi.org/10.1016/j.neuroimage.2006.04.182>.
- van Wingen, G.A., van Eijndhoven, P., Tendolkar, I., Buitelaar, J., Verkes, R.J., Fernández, G., 2011. Neural basis of emotion recognition deficits in first-episode major depression. *Psychol. Med.* 41 (07), 1397–1405, <http://dx.doi.org/10.1017/S0033297110002084>.
- Vasa, R.A., Pine, D.S., Thorn, J.M., Nelson, T.E., Spinelli, S., Nelson, E., et al., 2011. Enhanced right amygdala activity in adolescents during encoding of positively valenced pictures. *Dev. Cogn. Neurosci.* 1 (1), 88–99, <http://dx.doi.org/10.1016/j.dcn.2010.08.004>.
- Vergara, V.M., Mayer, A.R., Damaraju, E., Hutchison, K., Calhoun, V.D., 2016. The effect of preprocessing pipelines in subject classification and detection of abnormal resting state functional network connectivity using group ICA. *NeuroImage*, <http://dx.doi.org/10.1016/j.neuroimage.2016.03.038>.

- Vu, A.T., Jamison, K., Glasser, M.F., Smith, S.M., Coalson, T., Moeller, S., Auerbach, E.J., Ugurbil, K., Yacoub, E., 2017. Tradeoffs in pushing spatial resolution of fMRI for the 7T Human Connectome Project. *NeuroImage* 154, 23–32.
- Wang, A.T., Dapretto, M., Hariri, A.R., Sigman, M., Bookheimer, S.Y., 2004. Neural correlates of facial affect processing in children and adolescents with autism spectrum disorder. *J. Am. Acad. Child Adolesc. Psychiatry* 43 (4), 481–490, <http://dx.doi.org/10.1097/00004583-200404000-00015>.
- White, T., O'Leary, D., Magnotta, V., Arndt, S., Flaum, M., Andreasen, N.C., 2001. Anatomic and functional variability: the effects of filter size in group fMRI data analysis. *NeuroImage* 13 (4), 577–588, <http://dx.doi.org/10.1006/nimg.2000.0716>.
- Woolrich, M.W., 2008. Robust group analysis using outlier inference. *NeuroImage* 41 (2), 286–301.
- Woolrich, M.W., Behrens, T.E.J., Beckmann, C.F., Jenkinson, M., Smith, S.M., 2004. Multi-level linear modelling for FMRI group analysis using Bayesian inference. *NeuroImage* 21 (4), 1732–1747.
- Woolrich, M.W., Jbabdi, S., Patenaude, B., Chappell, M., Makni, S., Behrens, T., et al., 2009. Bayesian analysis of neuroimaging data in FSL. *NeuroImage* 45 (S), 173–186.
- Yue, Y.R., Loh, J.M., Lindquist, M.A., 2010. Adaptive spatial smoothing of fMRI images. *Stat. Interface* 3, 3–13.